Journal of Peptide Science, Vol. 3, 314–319 (1997)

SHORT COMMUNICATION

3D Structure of Kaliotoxin: Is Residue 34 a Key for Channel Selectivity?

MARGARIDA GAIRÍ[1], RÉGINE ROMI[2], IMMA FERNÁNDEZ[1]*, HERVÈ ROCHAT[2], MARIE-FRANCE MARTIN-EAUCLAIRE[2], JURPHAAS VAN RIETSCHOTEN[2], MIQUEL PONS[1] and ERNEST GIRALT[1]

[1]Departament de Química Orgànica, Universitat de Barcelona, Barcelona, Spain
[2]Laboratoire de Biochimie, UMR 6560, Ingénierie des Protéins, IFR Jean Roche, Faculté de Médecine Nord, Marseille, France

Received 13 February 1997
Accepted 3 March 1997

Abstract: Kaliotoxin (KTX) is a natural peptide blocker of voltage-dependent K^+ channels. The 3D structure of a truncated analogue of KTX (Fernández *et al.* (1994) *Biochemistry 33*, 14256–14263) was determined by NMR spectroscopy and showed significant differences from structures established for other related scorpion toxins. A recent publication with the structure of the complete toxin (Aiyar *et al.* (1995) *Neuron 15*, 1169–1181) did not confirm these differences. In this communication we report NMR data for KTX at pH 3.0, 5.5 and 7.2 and the 3D structure obtained from data at pH = 5.5. Complete KTX displays a folding similar to that of other toxins with an α-helix and a β-sheet linked by two disulphide bonds. The pK_a of His 34 is anomalously low (4.7–5.2 depending on the buffer) owing to its interaction with two Lys residues (including the essential Lys 27), the charged N-terminus and the side chain of Met 29. Charged residues are placed symmetrically with respect to an axis that approximately coincides with one of the principal components of the moment of inertia of the toxin. His 34, which occupies a well-defined position between two conserved Cys, is located on the centre of a layer of charged groups. Positively and negatively charged residues are found at the same position in related toxins. It is suggested that electrostatic effects modulate the distances between positive charges in flexible side chains, contributing to the fine tuning of the selectivity toward different channel subclasses and that the approximate coincidence between the moment of inertia and the charge axis facilitate the approach of the toxin to the channel. The very low pK_a of His 34 implies that it will be completely unprotonated at physiological pH. © 1997 European Peptide Society and John Wiley & Sons, Ltd.

J. Pep. Sci. 3: 314–319
No. of Figures: 3. No. of Tables: 1. No. of Refs: 22

Keywords: kaltoxin; NMR; K^+ channel blockers; scorpion toxin

Kaliotoxin (KTX) is a 38 residue peptide found in the venom of the scorpion *Androctonus mauretanicus mauretanicus* [1, 2]. KTX blocks voltage-dependent K^+ channels [3, 4] and is being used by our groups as a starting point for modifications aiming at increasing the selectivity towards different subclasses of K^+ channels. We had previously reported the structure at pH 3.0 of a truncated analogue of KTX lacking the C-terminal residue [5]. The structure of the complete toxin was subsequently published [4] and showed significant differences from our previous structure. In this paper we report our determination of the structure of complete KTX from

Abbreviations: AgTX, agiotoxin; ChTX, charybdotoxin; CVFF, consistent valence force field; DG, distance geometry; DQF-COSY, double quantum filtered correlation spectroscopy; IbTX, iberiotoxin; KTX, kaliotoxin; MgTX, Margatoxin; NTX, noxiustoxin; RMSD, root mean square difference; SA, simulated annealing; TOCSY, total correlation spectroscopy.

*Present address: Department of Biochemistry, University of Texas Southwestern Medical Center, 5323 Harry Hines Blvd, Dallas-TX 75235-9041, USA.
Address for correspondence: Prof. Miquel Pons, Departament de Química Orgànica, Facultat de Química, Universitat de Barcelona, Martí i Franquès, 1, E-08028 Barcelona, Spain.

CCC 1075-2617/97/040314-06

data obtained at pH 5.5 and the comparison of chemical shifts and NOE information obtained at pH 3.0, 5.5 and 7.2.

The structure of KTX was determined from 205 NOE and 23 dihedral angle (for Φ) constraints measured at pH = 5.5 and 298 K using a combined distance geometry and simulated annealing protocol. Interproton distance constraints consisted of 16 intra-residue, 97 sequential, 24 medium-range and 68 long-range NOEs. Stereospecific assignments were obtained for six pairs of β-methylene protons and one pair of γ-methyl groups of Val. Eighteen hydrogen-bonding distance restraints (two restraints for each of nine hydrogen bonds) were also included in the structure calculations. The final 18 structures had a backbone RMSD of 0.8 and good covalent geometry (Table 1). The first and last residues lack experimental constraints and are poorly defined. Superposition of backbone residues 2–37 gives an average RMSD of 0.59 Å. The percentage of Φ Ψ backbone dihedral angles in the most favourable regions of the Ramachandran plot is superior to 69% for all structures. The average is 77.2%. Most of the remaining backbone torsion angles fall in the additional allowed regions [6]. The final structures had an average of 2.8 violations between 0.1 and 0.2 Å per structure. The largest violation in any structure was 0.18 Å. Side chains are, in general, poorly defined, but some hydrophobic residues (I4, V6, L15, F25 and H34) are better defined owing to the larger number of NOEs observed for these side chains. Figure 1 shows a superposition of the final 18 structures of KTX.

KTX contains a well-defined three-strand β-sheet comprising residues R24-M29, K32- T36 and V2-C8. The N-terminal strand is interrupted by a bulge comprising residues N5 and V6. A helix extends from residue S11 to A21. The relative positions of the sheet and the helix are defined by conserved disulphide bonds between C8–C28, C14–C33 and C18–C35.

Figure 1 Superposition of 18 structures of kaliotoxin.

In addition to the data at pH 5.5 used for structure calculations, spectra of KTX were recorded and assigned at pH 3.0 and 7.2 in an unbuffered sample and at pH 5.5 in 50 mM deuterated sodium acetate. pH-induced chemical shift differences of NH protons are presented in Figure 2. The largest variations affect the N-terminal region (residues 2–7) and residues 28, 29, 30 and 33. Smaller changes are observed for residues 18–20 and in the loop connecting the helix and the sheet. Smaller changes affecting the same regions are observed for Cα

Table 1 Structural Statistics for 18 Kaliotoxin Structures after DG and SA Calculations

Average deviations from idealized covalent geometry, for all atoms excepting hydrogens			
(values in parentheses are the maximum deviations observed)			
Bond lengths (Å)		0.006° (0.03°)	
Bond angles (deg)		2.06 (13.7°)	
Peptide bond omega (deg)		0.30° (2.6°)	
Peptide bond improper (deg)		2.17° (8.4°)	
RMS deviations of atomic coordinates after superimposing 18 kaliotoxin structures			
(RMSD values are calculated vs. the average structure)			
Superimposed atoms	1–38 residues	2–37 residues	3–36 residues
All atoms	1.39 ± 0.14	1.28 ± 0.09	1.26 ± 0.09
Backbone (C^{α}, C,N,O)	0.80 ± 0.22	0.59 ± 0.09	0.55 ± 0.08
Backbone (C^{α}, C,N)	0.74 ± 0.24	0.52 ± 0.08	0.48 ± 0.07

protons (data not shown); however, the hydrogen bond between C35 NH and V2 CO is apparently maintained over the entire pH range and therefore the third strand is not lost at low pH. The ionization state of specific side chains was determined from chemical shifts changes in β-protons of Asp, γ-protons of Glu and aromatic protons of His. The chemical shift of the ^{2}H proton of H34 changes from 8.78 p.p.m. at pH 3 to 7.73 at pH 7.2 and the value of pH 5.5 is 7.87. The corresponding values for the ^{4}H proton are 7.54, 7.10 and 7.20. The estimated pK_a is 4.7. The chemical shifts at pH 5.5 in 50 mM sodium acetate are 8.10 and 7.28 for the ^{2}H and ^{4}H protons respectively. The chemical shifts of other protons were unaffected by ionic strength. Assuming that the limiting chemical shifts were also not affected by the buffer, the pK_a of H34 in 50 mM acetate would be about 5.2. NOEs measured at the three pH values were very similar in number and intensity except for some NH protons that were exchanging fast at pH 7.2.

The 3D structure of KTX at pH 5.5 is closely similar to that of other related toxins and significantly different from our previously determined structure for KTX(1–37) at pH 3.0. An analysis of the 3D structure of KTX at pH 5.5 indicates that H34 is about 50% exposed to solvent and is surrounded by charged residues: K27, K32 and G1. Additionally, the side chain of H34 is in contact with that of M29. These interactions, all of which are supported by the observation of NOESY cross-peaks, can explain the low pK_a of H34 by a combination of repulsive electrostatic interactions in the charged form and favourable van der Waals contacts in the uncharged form. The sensitivity to ionic strength points to a dominant role for the electrostatic effects. A low pK_a of 5.28 has been reported for H21 of charybdotoxin [7]. However, the two residues are not homologous and the origin of the effect is probably different in the two toxins. In both cases, however, histidine is expected to be completely unprotonated at pH 7 thus affecting the global charge of the molecule.

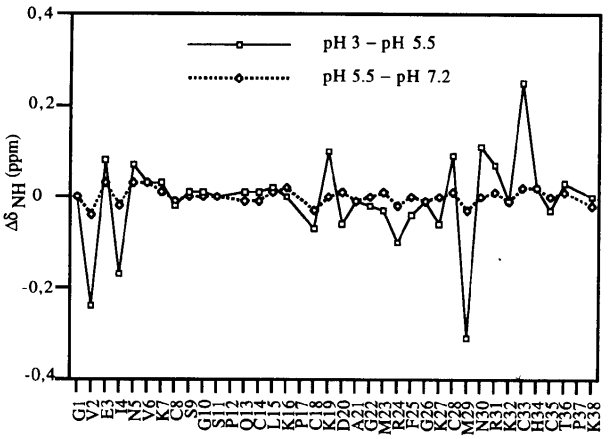

Figure 2 Chemical shift differences for NH protons of kaliotoxin between pH 3.0 and 5.5 (squares) and between pH 7.2 and 5.5 (triangles).

The H34 side chain is participating also in a bifurcated hydrogen bond with the carbonyl group of M29, which is hydrogen bonded across the β-sheet with K32 NH. Finally, H34 is facing E3 when the third strand is well formed and an electrostatic interaction across the β-sheet is expected when both groups are charged. However, given the low pK_a of H34 this interaction will be effective at most in a narrow pH range around pH 3–5. In the closely related agitoxin 2 [8] position 3 is occupied by proline but the third strand is equally well formed, further suggesting that the electrostatic interaction between His and Glu is not necessary for the stability of the β-sheet.

The distribution of charges in KTX shows a remarkable symmetry and is located in three layers around an axis that passes very close to the centre of mass of the molecule and nearly parallel to one of the principal components of the moment of inertia. The first layer contains K27, K32 and the N-terminal amino group, the second layer is composed of R31, R24, K7 and K38 and approximately coincides with the plane formed by the other two principal moments of inertia. The third layer, formed by K16 and K19, is located on the opposite side of the above plane. H34 is located very close to the centre of the first layer and of the symmetry axis just mentioned (Figure 3). Position 34 is part of the β-sheet and is flanked by strictly conserved C33 and C35 and therefore the orientation of its side chain is expected to be also highly conserved. However position 34 (or the equivalent homologous position) is not conserved and is occupied by His in KTX and AgTX [10], by Arg in ChTX [11] and IbTX [12], by Lys in NTX [13] and MgTX [14], by Asp in KTX2 [15] and by Glu in Leiurotoxin [16] and PO5-NH_2 [17]. All of these toxins for which the 3D structure is available from the Protein Data Bank, share an approximately cylindrical distribution of charges around an axis which coincides with the principal component of the moment of inertia perpendicular to the plane of the β-sheet, although some toxins (like PO5-NH_2) have only two layers of charged groups. Distances between the Cα atoms of the positively charged residues in the layer located around residue 34 or

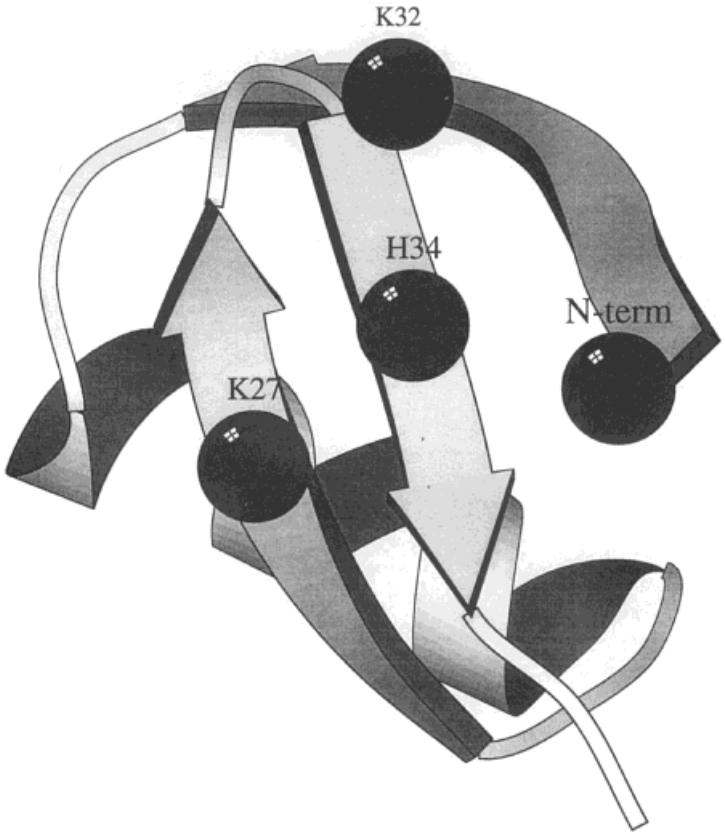

Figure 3 MolScript [9] plot of kaliotoxin showing the distribution of positively charged residues around His 34 in the face of the β-sheet that interacts with the channel. Black spheres mark the position of β-carbons, except for the N-terminal residue in which the α-carbon is highlighted.

its equivalent are similar in all toxins but the distances between the actual charges are not well determined in solution owing to the flexibility of the corresponding side chains. The strong electrostatic interaction, manifested in KTX by the strong pK_a shift, should however have a strong influence on the actual diameter of the charge belt around residue 34. Negatively charged residues, such as those of KTX2, Leiurotoxin and PO5-NH_2 will tend to contract the charged belt. Positively charged residues, like those of ChTX, IbTX, MgTX and NTX, will tend to increase this diameter by the mutual repulsion between charged residues but because of the different length of the side chain Lys and Arg could have a different effect. In fact the situation in ChTX is possibly better described by considering K34 as part of the charge ring instead of its centre. Finally, His being uncharged at neutral pH will probably have an intermediate effect. It is interesting that in the toxins in which the N-terminal amino group participates in this charge belt (like KTX and AgTX) the N-terminal residues form a well-defined strand of the β-sheet while in toxins in which the N-terminal does not bear a charge (like ChTX and IbTX) the charged belt if formed by Lys and Arg residues and the third strand is not well defined in the structures.

The coincidence between the axis around which the charges are approximately distributed and one of the principal components of the moment of inertia of the molecule is probably not fortuitous. Free toxins will be rotating in solution providing a contribution to the kinetic energy of $1/2I\omega^2$. Considering a mass of 4000 dalton, a radius of 13 Å, a correlation of 10^{-10} s and a single layer of water molecules around the protein, this contribution is around 0.1 kcal/mol. Rotational entropy loss due to toxin binding is proportional to this quantity. This value could be higher as a consequence of extended hydration of charged residues. As the toxin approaches the channel it will interact electrostatically with negatively charged residues placed symmetrically around the channel axis, a consequence of its tetrameric nature. If the positive charges in the toxin are placed forming an approximately circular array

binding will be facilitated. The presence of two charged residues in the opposite side of the molecule could also contribute to the approach of the toxin to the channel. Rapid rotation around the long axis of the molecule has the lowest associated energy but a positively charged surface would always be directed toward the channel facilitating the approximation.

While the conservation of a number of residues in different toxins clearly points to their relevant role for structural integrity (e.g. the six Cys residues that globally stabilize the fold and G26 in the interface between the helix and the sheet) or general binding to the channel (e.g. R24, K27 and K32 in KTX or AgTX), the quest for selectivity should be focused on structurally well-defined residues with a large variability between toxins with different selectivity. Position 34 in KTX has these characteristics. It is suggestive that the residues at position 34 in KTX and homologous positions in other toxins are well conserved within each structural subfamily of toxins but are different among these families. Systematic mutational studies at this position could help to find new analogue toxins with improved selectivity.

EXPERIMENTAL

KTX was synthesized by solid-phase methods, purified and characterized as previously reported [2]. Two NMR samples were prepared: the first one was about 3 mM in 90% H_2O/10% D_2O or 100% D_2O. With this sample spectra were recorded at pH = 3.0, 5.5 and 7.2. The pH was adjusted by the addition of small amounts of NaOH or HCl. The second sample was about 3 mM peptide in 50 mM deuterated sodium acetate buffer (pH = 5,5) in 90% H_2O/10% D_2O. Dioxane was used as internal reference. Assignment followed from comparison of TOCSY (72 ms mixing time using MLEV) and NOESY spectra (150 and 400 ms mixing time) using well-established methodology [18]. Spectra were recorded on a Bruker DMX-500 instrument and Watergate [19] was used for water suppression. Semi-quantitative information on $^3J_{NH\alpha H}$ was obtained from DQF-COSY spectra. Proton–deuterium exchange experiments were carried out at pH 3.0 and followed using short TOCSY spectra. NOESY spectra used for structure calculations were recorded at 298 K with a mixing time of 150 ms. Cross-peaks were classified in three groups (strong, medium and weak) that were translated to upper distance limit restraints of 3, 4 and 5 Å respectively. For the strongest $d_{\alpha N}$ and d_{NN} sequential cross-peaks the limit was set to 2.8 Å. Pseudoatoms were used when diastereotopic protons could not be distinguished and the corresponding corrections in the restraints were applied [18]. ϕ angle constrainst derived from $^3J_{NH\alpha H}$ were incorporated according to the following rules: $-120^\circ \pm 25^\circ$ if $^3J_{NH\alpha H} > 9$ Hz, $-120^\circ \pm 35^\circ$ if 9 Hz $> {}^3J_{NH\alpha H} > 8$ Hz and $-70^\circ \pm 35^\circ$ if $^3J_{NH\alpha H} < 6$ Hz. Information from hydrogen bonds was introduced only in well-defined secondary structure elements unequivocally identified from a typical NOE pattern and in which the amide proton was protected from exchange by deuterium.

Structures were calculated using a combination of distance geometry (DGII program [20]) and simulated annealing (Discover program [21]). The consistent valence force field (CVFF) was used for SA calculations. The programs are commercially available from Molecular Simulation Inc. (San Diego, CA). During DG calculations disulphide bonds were introduced only as distance constraints [22] between S^i–S^j (1.9 Å $< r <$ 2.2 Å), S^i–C^j_β (2.9 Å $< r <$ 3.5 Å), C^i_β–C^j_β (2.9 Å $< r <$ 4.5 Å) and C^i_α–C^j_α (3.0 Å $< r <$ 6.8 Å). A quartic potential was used instead of Coulombic and Lennard-Jones terms in the force field and all the residues were considered in their uncharged state during the calculations.

Fifty structures were initially generated using DG. From these, the 35 having five or less distance violations lower than 0.1 Å were selected. In this set true covalent disulphide bonds were introduced and the resulting structures, after unrestrained energy minimization, were used as a starting point for SA calculations. These consisted of 10 ps of dynamics at 1000 K during which NOE and dihedral terms in the potential were scaled to their maximal values (50 kcal/mol/Å^2 and 60 kcal/mol/rad^2 respectively) followed by cooling to 300 K during 10 ps and 5 ps of restrained dynamics at 300 k. The resulting structures were energy-minimized. The best 18 structures were selected to have the lowest total energy (159–174 kcal/mol) and distance violations. These structures have been deposited with the Brookhaven Protein Data Bank (ident code 2KTX).

Acknowledgements

This work was supported by funds from CICYT (PB94-0924 and PB95-1131) and Generalitat de Catalunya (Centre de Referència en Biotecnologia and Grup Consolidat). M. G. holds a fellowship from Bruker Spectrospin. We thank Dr Thomas Haack for help in preparing the MolScript Drawing. We acknowledge the use of the NMR facilities of the Serveis Científico-Tècnics de la Universitat de Barcelona.

REFERENCES

1. M. Crest, G. Jacquet, M. Gola, H. Zerrouk, A. Benslimane, H. Rochat, P. Mansuelle and M.-F. Martin-Eauclaire (1992). Kaliotoxin, a novel peptide inhibitor of neuronal BK-type Ca^{2+}-activated K^+ channels characterized from *Androctonus mauretanicus mauretanicus* venom. *J. Biol. Chem. 267*, 1640–1647.
2. R. Romi, M. Crest, M. Gola, F. Sampieri, G. Jacquet, H. Zerrouk, P. Mansuelle, O. Sorokine, A. van Dorsselaer, H. Rochat, M.-F. Martin-Eauclaire and J. van Rietschoten (1993). Synthesis and characterization of kaliotoxin. Is the 26–32 sequence essential for potassium channel recognition? *J. Biol. Chem. 268*, 26302–26309.
3. S. Grissmer, A. N. Nguyen, J. Aiyar, D. C. Hanson, R. J. Mather, G. A. Gutman, M. J. Karmilowicz, D. D. Auperin and K. G. Chandy (1994). Pharmacological characterization of five cloned voltage-gated K^+ channels, types Kv1.1, 1.2, 1.3, 1.5 and 3.1, stably expressed in mammalian cell lines. *Molec. Pharmacol. 45*, 1227–1234.
4. J. Aiyar, J. M. Withka, J. P. Rizzi, D. H. Singleton, G. C. Andrews, W. Lin, J. Boyd, D. C. Hanson, M. Simon, B. Dethlefs, C. Lee, J. E. Hall, G. A. Gutman and K. G. Chandy (1995). Topology of the pore-region of a K^+ channel revealed by the NMR-derived structures of scorpion toxins. *Neuron 15*, 1169–1181.
5. I. Fernández, R. Romi, S. Szendeffy, M.-F. Martin-Eauclaire, H. Rochat, J. van Rietschoten, M. Pons and E. Giralt (1994). Kaliotoxin(1–37) shows structural differences with related potassium channel blockers. *Biochemistry 33*, 14256–14263.
6. A. L. Morris, M. W. MacArthur, E. G. Hutchinson and J. M. Thornton (1992). Stereochemical quality of protein structure coordinates. *Proteins: Structure, Func. Genet. 12*, 345–364.
7. T. R. Dyke, B. M. Duggan, M. W. Pennington, M. E. Byrnes, W. R. Kem and R. S. Norton (1996). Synthesis and structural characterisation of analogues of the potassium channel blocker charybdotoxin. *Biochim. Biophys. Acta 1292*, 31–38.
8. A. M. Krezel, C. Kasibhatla, P. Hidalgo, R. MacKinnon and G. Wagner (1995). Solution structure of the potassium channel inhibitor agitoxin 2: Caliper for probing channel geometry. *Protein Sci. 4*, 1478–1489.
9. P. J. Kraulis (1991) MOLSCRIPT: a program to produce both detailed and schematic plots of protein structures. *J. Appl. Crystallogr. 24*, 946–950.
10. M. L. García, M. García-Calvo, P. Hidalgo, A. Lee and R. MacKinnon (1994). Purification and characterization of three inhibitors of voltage-dependent K^+ channels from *Leiurus quinquestriatus* var. *hebraeus venom. Biochemistry 33*, 6834–6839.
11. G. Giménez-Gallego, M. A. Navía, J. P. Reuben, G. M. Katz, G. J. Kaczorowski and M. L. García, (1988). Purification, sequence, and model structure of charybdotoxin, a potent selective inhibitor of calcium-activated potassium channels. *Proc. Natl. Acad. Sci. USA 85*, 3329–3333.
12. A. Gálvez, G. Giménez-Gallego, J. P. Reuben, L. Roy-Contancin, P. Feigenbaum, G. J. Kaczorowski and M. L. García, (1990). Purification and characterization of a unique, potent, peptidyl probe for the high conductance calcium-activated potassium channel from venom of the scorpion *Buthus tamulus. J. Biol. Chem. 265*, 11083–11090.
13. L. D. Possani, B. M. Martin and I. B. Svendsen (1982). The primary structure of noxiustoxin: A K^+ channel blocker peptide purified from the venom of the scorpion *Centruroides noxius* Hoffmann. *Carlsberg Res. Commun. 47*, 285–289.
14. M. García,-Calvo, R. J. Leonard, J. Novick, S. P. Stevens, W. Schmalhofer, G. J. Kaczorowski and M. L. García (1993). Purification, characterization, and biosynthesis of margatoxin, a component of *Centruroides margaritatus* venom that selectively inhibits voltage-dependent potassium channels. *J. Biol. Chem. 268*, 18866–18874.
15. F. Laraba-Djebari, C. Legros, M. Crest, B. Céard, R. Romi, P. Mansuelle, G. Jacquet, J. van Rietschoten, M. Gola, H. Rochat, P. E. Bougis and M.-F. Martin-Eauclaire (1994). The kaliotoxin family enlarged. Purification, characterization and precursor nucleotide sequence of KTX2 from *Androctonus Australis* venom. *J. Biol. Chem. 269*, 32835–32843.
16. G. G. Chicchi, G. Giménez-Gallego, E. Ber, M. L. García, R. Winquist and M. A. Cascieri (1988). Purification and characterization of a unique, potent inhibitor of apamin binding from *Leiurus quinquestriatus hebraeus* venom. *J. Biol. Chem. 263*, 10192–10197.
17. J. M. Sabatier, H. Zerrouk, H. Darbon, K. Mabrouk, A. A. Benslimane, H. Rochat, M.-F. Martin-Eauclaire and J. van Rietschoten (1993). PO5, a new leiurotoxin I scorpion toxin: Synthesis and structure–activity relationships of the a-amidated analog, a ligand of Ca^{2+}-activated K^+ channels with increased affinity. *Biochemistry 32*, 2763–2770.
18. K. Wüthrich: *NMR of Proteins and Nucleic Acids*, Wiley, New York 1986.
19. M. Piotto, V. Saudek and V. Sklenar (1992). Gradient-tailored excitation for single-quantum NMR spectroscopy of aqueous solutions. *J. Biomol. NMR 2*, 661–665.
20. T. F. Havel, I. D. Kuntz and G. M. Crippen (1983). The theory and practice of distance geometry. *Bull. Math. Biol. 45*, 665–720.
21. R. D. Feinstein, A. Polinsky, A. J. Douglas, C. Magnus, C. F. Beijer, R. K. Chadha, E. Benedetti and M. Goodman (1991). Conformational Analysis of the Dipeptide Sweetener Alitame and Two Stereoisomers by Proton NMR, Computer Simulations, and X-ray Crystallography. *J. Am. Chem. Soc. 113*, 3467–3473.
22. N. Srinivasan, R. Sowdhamini, C. Ramakrishnan and P. Balaram (1990). Conformations of disulfide bridges in proteins. *Int. J. Peptide Res. 36*, 147–155.